JOURNAL OF MATERIALS SCIENCE 20 (1985) 2159–2168

The interface region in squeeze-infiltrated composites containing δ-alumina fibre in an aluminium matrix

G. R. CAPPLEMAN*, J. F. WATTS, T. W. CLYNE‡
Department of Materials Science and Engineering, University of Surrey, Guildford, Surrey, UK

This paper examines the nature of the interfaces formed between fine, δ-alumina fibres and aluminium-based matrices. Alloys containing magnesium and silicon have been employed, as well as high-purity aluminium. The fabrication process involved high-pressure melt infiltration of a fibrous preform. It has been found that no detectable interfacial reaction product is formed in these systems, although there is in some cases evidence of a limited exchange of magnesium between melt and fibre surface. It is concluded, both from measurements and from process analysis, that any distinct chemical reaction product formed at the interface between fibre and matrix must be limited in extent to the atomic monolayer level.

1. Introduction

In metal matrix composites (MMC), as in their polymer counterparts, the interface between the matrix and the reinforcing phase can play a key role in determining the mechanical properties of the system. This is because, in order to optimize properties such as stiffness and tensile strength, transfer of load from the matrix to the reinforcing phase is necessary. The present work is concerned with the interface between an aluminium, Al–Mg, or Al–Si alloy matrix and δ-Al_2O_3 fibres. These fibres are fine, with a mean diameter around 3 μm, and for MMC purposes they are milled and graded to give an average length of about 500 μm.

The fibre, known as Saffil§ alumina fibre, RF grade, has a polycrystalline structure in which the predominant phase is δ-alumina [1, 2]. The material also contains about 3 to 4 wt% SiO_2, which serves to stabilize the δ-structure and to inhibit coarsening of the fine (50 nm) crystallite size. This silica is dispersed throughout the fibre section, but also tends to become slightly concentrated at grain boundaries and free surfaces. This effect is enhanced on excessive heating, when small crystallites of mullite ($3Al_2O_3 \cdot 2SiO_2$) may appear. It is thought that, in the normal state, the enrichment may extend to a composition close to that of mullite, although no phase separation is detectable. Thus it is a thin silica-rich layer on the surface of the fibre which is in contact with the matrix material during fabrication, rather than pure δ-alumina. The thickness of this surface layer is not accurately known, but estimates based on grain size and silica level (and assuming a surface concentration of SiO_2 close to that of mullite) suggest a figure of around 1 nm.

Previous work with aluminium/alumina systems has shown liquid infiltration to be a promising fabrication route [3–5], although all types of processing have been hampered by the poor intrinsic wetting characteristics of the system [6–10]. In an attempt to overcome this, fibre coatings [11] or alloy additions [12] have been used to enhance the formation of a chemical bond. Alloy additions have in some cases involved the use of lithium, which forms $Li_2O \cdot 5Al_2O_3$ at the

*Present address: Department of Metallurgy and Materials Science, Pembroke Street, Cambridge, UK.
‡Present address; Unilever Research, Colworth House, Sharnbrook, Bedfordshire, UK.
§Saffil is a trademark of Imperial Chemical Industries plc for alumina fibres.

0022–2461/85 $03.00 + .12

fibre/matrix interface, although other transition metals have been suggested as additions to form aluminates isostructural with the spinel $MgO \cdot Al_2O_3$. More specifically, work with the DuPont α-Al_2O_3/aluminium system [13–16] has indicated that such spinels do form at that particular fibre/matrix interface.

The interface being investigated in the present work differs from those in the above studies in at least three important respects. Firstly, the fabrication process is more rapid, with very transient melt/fibre/atmosphere contact and a short melt/fibre residence time. Secondly, the small diameter of the fibre means that we are concerned with relatively large specific surface areas. Finally, the metstable δ-alumina structure is not one that has been extensively studied in the context of MMC behaviour.

2. Experimental procedure

Composites were fabricated using a squeeze-infiltration technique described elsewhere [17], which has been termed "pressure-assisted network infiltration to form composites" (PANIC). A fibre preform of diameter 60 mm and thickness 15 mm was placed in a die preheated to 550 K and infiltrated with liquid metal. This was either high-purity aluminium or alloys containing silicon or magnesium (see Table I for compositions), superheated by about 150 K and injected by means of a ram initially travelling at about 9 mm sec^{-1}, with a pressure setting of 25 to 30 MPa. The preforms had a fibre volume fraction f_{fib} of approximately 0.18, and incorporated 5 wt% of silica binder in addition to the silica in the fibre. Previous work [17] had indicated the level and nature of the binder to be of little importance in terms of the final microstructure, although it affected the handling properties of the preform. Process analysis and measurements have shown that, under the conditions employed, the time for the melt to infiltrate the pad is very short (~ 1 sec). The interface between the fibres and the alloy has been examined by optical microscopy, transmission electron microscopy (TEM) and X-ray photoelectron spectroscopy (XPS). Specimens were prepared for TEM by lapping transverse sections to about 30 μm thickness on metallographic paper and then thinning small pieces of the specimen with an ion beam. This gave a specimen with some regions thin enough for TEM analysis, and the interface was examined on a JEOL 200 CX transmission electron microscope using an accelerating voltage of 160 kV.

TABLE I Chemical compositions of matrix phases used in this work

Alloy	Composition
Aluminium	99.999 % pure
Al–Mg	Mg 9.5 to 11.0%, Fe 0.35% max, Si 0.25% max, Al to 100%
Al–Si	Si 10.0 to 13.0%, Fe 0.6% max, Mn 0.5% max, Al to 100%

Specimens were prepared for XPS by dissolving away the matrix of a 10 mm x 10 mm x 2 mm piece of composite in a 10% solution of iodine in methanol at 50° C. This was carried out under anaerobic conditions, which eliminated the possibility of the formation of metal hydroxides in the stripping solution. This was achieved by the use of an enclosed glass stripping rig employing oxygen-free nitrogen as an inert environment and a means of transporting stripping and washing solutions. Design of the apparatus closely followed the original philosophy of Vernon, Wormwell and Nurse [18]. The fibres were then pressed into indium foil for XPS analysis.

X-ray photoelectron spectra were recorded using a VG Scientific ESCA3 Mk II electron spectrometer, with Al$K\alpha$ radiation ($h\nu = 1486.6$ eV) at an analyser pass energy of 50 eV; the vacuum in the analyser during analysis was approximately 10^{-9} mbar (10^{-7} N m^{-2}). During acquisition, and for subsequent data analysis, the spectrometer was controlled by a VG 3040 data system based on a DEC PDP8e computer. Quantification of the XPS was achieved using peak areas, with a linear background-subtraction, and the appropriate sensitivity factors.

Al$K\alpha$ radiation was employed in preference to Mg$K\alpha$ to enable excitation of the Mg–1s core level for the specimens prepared from the Al–Mg composite, and for the other samples to ensure consistency of results, especially the escape depths of the various photoelectrons. The examination of aluminium-containing materials in Al$K\alpha$ radiation does, however, lead to the excitation of an Al–KLL Auger peak at approximately the same position as the Si–2p photopeak [19]. For this reason the work described in this paper has examined the Si–2s core level at a binding energy of approximately 150 eV.

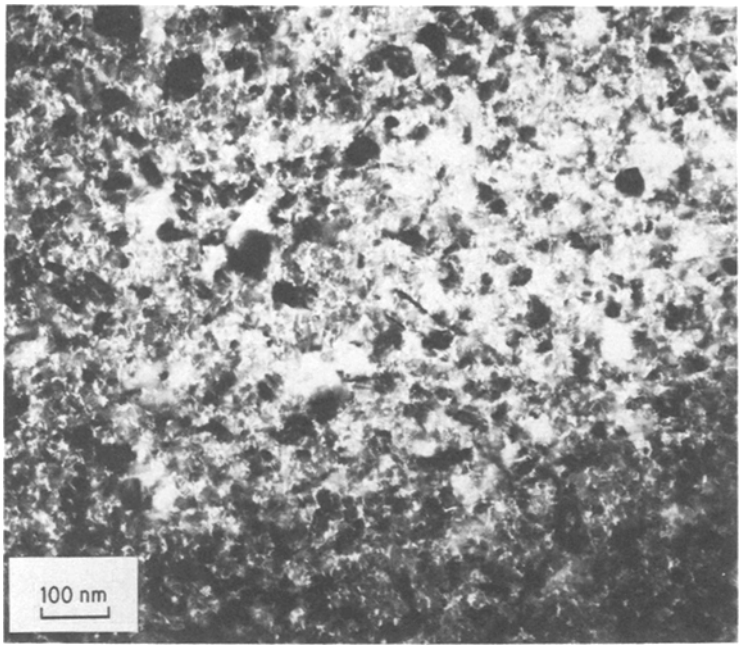

Figure 1 Bright-field TEM micrograph of a virgin fibre, showing the crystallite structure.

3. Results and discussion

3.1. Analysis of fibres

The structure of the virgin fibre is shown in the TEM image of Fig. 1, which illustrates the crystallite size and shape. A typical microstructure of a squeeze-formed composite of high purity Al/δ-Al_2O_3 is shown in Fig. 2. This demonstrates the absence of porosity in the composite as a whole, and also the intimate contact between fibre and matrix. It might be argued that spinel formation is unlikely in this case in view of the absence of potential divalent ions in the liquid, although formation of the $AlO \cdot Al_2O_3$ structure postulated by Brennan and Pask [7] might conceivably be a possibility. However, if spinel formation were expected it would be most likely with the alloy containing 10 wt % Mg. Extensive optical metallography and TEM were carried out on composites fabricated using this alloy, but in no case was an intermediate phase between the fibres and the matrix clearly evident. The bright-field TEM image in Fig. 3 indicates that any third phase formed between the matrix and reinforcing fibre must have been on an extremely fine scale, if present at all. Associated with any intermediate phase on the fibre should have been a change in

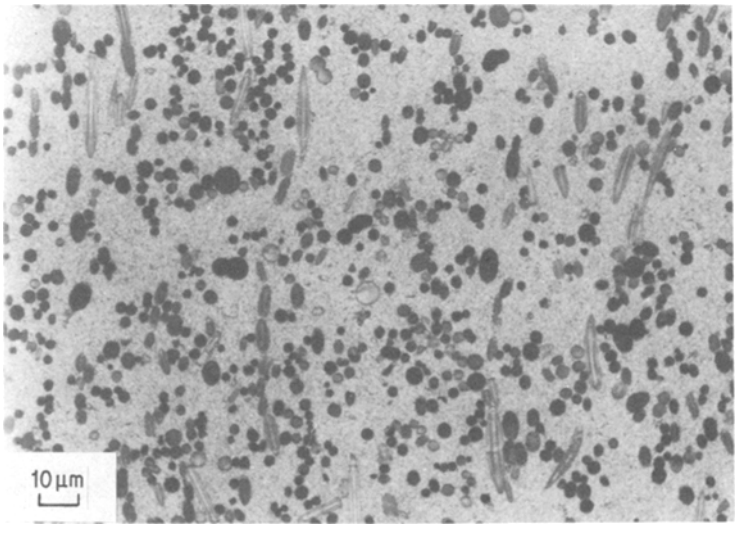

Figure 2 Typical composite microstructure of a squeeze-formed composite of high-purity aluminium and Saffil (δ-Al_2O_3) fibres.

Figure 3 TEM bright-field image of the interface region between fibre and matrix in a composite containing 10 wt % Mg.

the chemistry of the fibre surface itself. In view of the need for chemical information at very high depth resolution, the fibre surface was examined using XPS. This is a surface-specific technique involving analysis of the top 2 to 5 nm of the specimen [20]; the photoelectron escape depth depends primarily on the electron kinetic energy, and hence on the energy levels of the shells concerned.

Quantitative XPS data are given in Table II for fibres in the virgin state and after extraction from composites. Also shown are data for fibres treated with hydrofluoric acid to remove the surface (silica-rich) layer. Analysis of the virgin material indicates an appreciable level of silicon, which is associated with the silica enrichment at the surface. The high silicon level from the HF-treated fibre in the preform, on the other hand, comes from the silica binder. This tends to accumulate at fibre contact points in the preform. The exact fate of the binder during melt infiltration is not yet clear, but it appears to be eliminated during extraction of fibre from the composite. The analyses have been normalized to exclude adventitious carbon, present at a fairly low level on all surfaces. Traces of iodine (from the stripping solution) were also detected.

TABLE II XPS surface analyses of as-received fibres and those extracted from Al–Si and Al–Mg alloys

Fibre type	Composition (at %)			
	Al	Si	Mg	O
Virgin fibre	23.6	5.7	0.0	70.7
HF-treated fibre + binder (in preform)	18.7	10.2	0.0	71.1
Extracted (Al–Mg alloy)	18.2	5.5	6.3	70.0
HF-treated and extracted (Al–Mg alloy)	21.1	0.0	0.0	62.1
Extracted (Al–Si alloy)	12.1	25.9	0.0	62.1

The silicon 2*s* spectra from the virgin fibres and from those extracted from the magnesium-bearing composite are both centred at approximately 154 eV, indicative of SiO_2 (Figs. 4a and 5a). There is, however, a diminution of aluminium for the extracted fibre as a result of the incorporation of magnesium into the interfacial layer at about the same concentration as the silicon. The spectrum obtained from these fibres [17] shows Mg^{2+} peaks at 1305 eV (1*s* photoelectrons), 300 to 400 eV (Auger *KLL* electrons) and 52 and 89 eV (2*p* and 2*s* photoelectrons). The ratio of the intensity of the Mg–1*s* peak to that of the Mg–2*s* is about 14, which may be compared with values of 20 and 22 recorded [21, 22] from a clean magnesium fluoride standard. This discrepancy may be a result of adventitious carbon on the surface, which would attenuate the low-energy Mg–1*s* electron (1305 eV binding energy, 182 eV kinetic energy) more effectively than the energetic Mg–2*s* electron (89 eV binding energy, 1398 eV kinetic energy). By manipulation [23] of the Beer–Lambert equation, it is possible to estimate the thickness of carbon necessary to give the observed reduction in

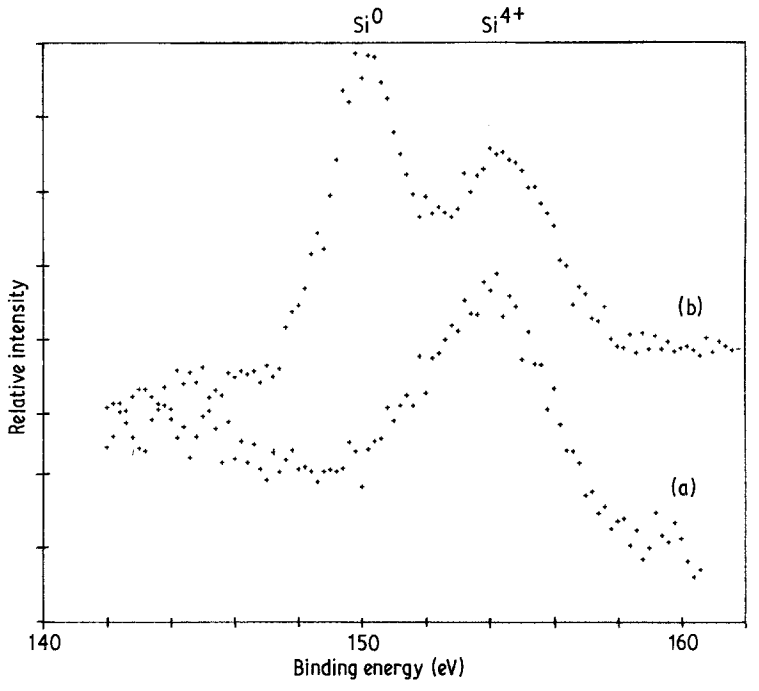

Figure 4 Silicon 2*s* XPS spectra of fibres extracted from (a) pure aluminium matrix (those from Al–Mg alloy and virgin fibre are very similar), showing SiO_2 at 154 eV; (b) Al–Si matrix, showing a substantial additional contribution from elemental silicon (150 eV).

the Mg–1*s*/Mg–2*s* ratio, assuming the magnesium-enriched layer to be infinitely deep ($\gg$ 5 nm). The result obtained is 0.17 nm, which might be conceivable for a discontinuous overlayer, but is much less than the figure of about 0.7 nm expected [24] for a uniform coating on a sample of the type in question. The Mg–1*s*/Mg–2*s* ratio expected for this thickness of carbon layer would be about 9.9.

The most likely explanation for the discrepancy is that the depth of the magnesium-enriched layer is not infinite. While the Beer–Lambert expression is strictly applicable only to planar surfaces, it may be used here to estimate the thickness of this layer. The analysis depth for the escaping photoelectrons ($\sim 3\lambda$, where λ is the inelastic mean free path) is about 1.5 nm for the Mg–1*s* case and

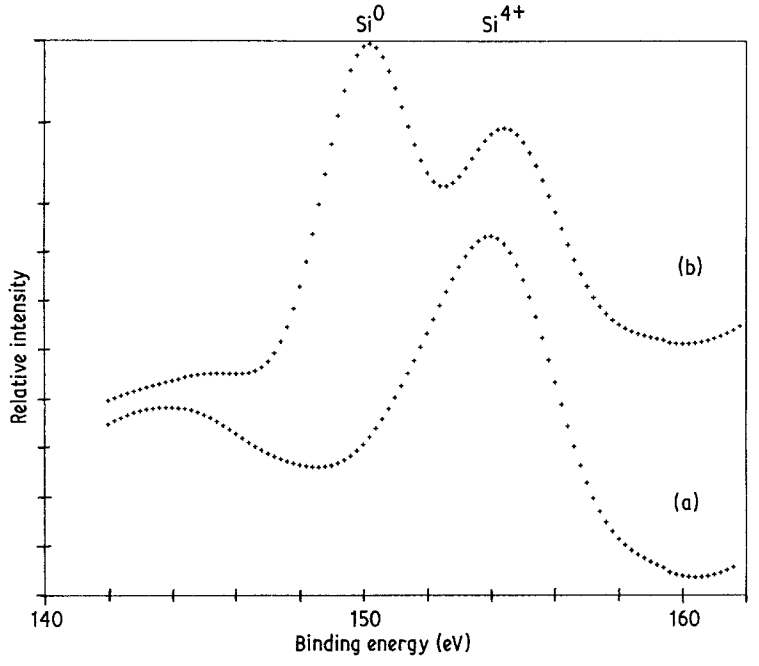

Figure 5 Data of Fig. 4, after the application of a least-squares smoothing routine.

5.5 nm for Mg–2*s* [25], If magnesium enrichment is present to a depth less than this latter figure, the Mg–1*s*/Mg–2*s* ratio will increase. In fact, it is possible to calculate (taking account of the carbon-layer attenuation effect) the depth of enrichment which would be consistent with the observed ratio: this turns out to be 0.5 to 1.0 nm. It would thus appear likely that, although magnesium enters into the surface of the fibres (possibly into vacant sites in a defective lattice), rather than being present as an overlayer (a conclusion supported by the constancy of the silicon signal for virgin and standard Al–Mg extracted cases), the magnesium penetration is limited to a few atomic layers. It is suggestive that this depth may be of the same order as that of silica-enrichment, implying possibly a crystal structure of mullite in the surface of the virgin fibre.

The HF-treated fibres from the Al–Mg composite exhibit no magnesium incorporation of the type described above. Silicon is also absent, although the corresponding virgin preform contained a relatively high level. This is undoubtedly attributable to the silica binder. During dissolution in the iodine solution, the binder residues (which are not chemically bonded to the fibre surface) are swept away. The absence of silicon for the extracted fibre demonstrates that removal of the enriched layer was successful: the corresponding absence of magnesium thus adds weight to the above hypothesis that entry of magnesium into the surface layers is dependent on the presence of silica in those layers.

Turning now to those fibres extracted from the silicon-containing matrix, the concentration of silicon is much higher than for the other cases. Inspection of the Si–2*s* spectrum from this material (Fig. 4b) shows the major spectral component to be centred at 150 eV, and this is ascribed to elemental silicon (Si^0). There is also the component from the SiO_2 phase as in Fig. 4a. Comparison of these spectra is facilitated by presentation in the smoothed form shown in Fig. 5. The Si^0 peak is probably a result of silicon precipitates (present in the as-cast alloy) forming on the fibre surface. It has been noted [17] that the fibres can apparently act as preferential substrates for nucleation of some silicon precipitates, which apparently then adhere to the fibres to some extent during extraction. Thus the silicon 2*s* spectrum of the fibres extracted from the silicon-containing alloy has contributions from three types of material; Si^0 from the precipitates discussed above, Si^{4+} from the oxidized silicon inevitably present at the surface of these precipitates, and Si^{4+} originally present on the fibre surface.

The conclusions that can be drawn from these spectra are thus as follows. The SiO_2 in the surface layers of the fibre has not been chemically changed by being in contact with the liquid metal matrix, as the silicon photopeaks only show elemental silicon when it is present in the alloy. The only major change which takes place on the fibre surface is when Al–Mg alloy is used as the matrix: in this case Mg^{2+} appears to be incorporated into the lattice of the fibre surface.

It is thought that SiO_2 may be present on the surface of the fibre in the form of the mullite phase ($3Al_2O_3 \cdot 2SiO_2$): this has a structure consisting of chains of aluminium octahedra parallel to the *z*-axis, crosslinked by tetrahedra containing both silicon and aluminium. It may be regarded as a disordered phase intermediate between two ordered phases, sillimanite and andalusite [26], with partial replacement of silicon by aluminium and a shift of some of the tetrahedral cations into open sites. Mullite can exhibit a variation in composition from $3Al_2O_3 \cdot 2SiO_2$ (containing 60 mol% Al_2O_3) to $2Al_2O_3 \cdot SiO_2$ (with 67 mol% Al_2O_3). It therefore seems feasible that, in the cases of high purity aluminium and the Al–Si alloys, some oxidation of the aluminium might have taken place at the surface of the fibre; the alumina thus produced could then have been incorporated into the mullite phase. This would account for the fact that no interface phase is visible in TEM, as any reaction of this nature would necessarily take place over the few atomic layers where mullite is present. The possibility remains, of course, that there was no chemical reaction of any nature in these cases, and that the bonding is merely the result of intimate physical contact.

In the case of magnesium-containing alloys it is possible that $MgO \cdot Al_2O_3$ (spinel) is formed at the surface of the fibres in the presence of SiO_2. The mullite structure has close similarities to the sillimanite structure, in which it is interesting to note that there are chains of AlO_6 octahedra and $(Si, Al)O_4$ tetrahedra parallel to the *c*-axis, whilst similar chains run in the ⟨1 1 0⟩ directions in spinel. It is therefore possible that this spinel would form, but again only over the few atomic

layers where mullite has previously been present. The absence of zero-valent silicon in cases where slight magnesium absorption has taken place is particularly interesting, and leaves in some doubt the exact mechanism by which Mg^{2+} ions have been incorporated into the lattice. However, although silica reduction by straight cationic exchange might have been the expected mechanism, it should be mentioned that the precise crystallography of the fibre surface remains uncertain, leaving the possibility that Mg^{2+} ions are occupying vacant sites in a defective lattice. This suggestion raises the question of charge transfer, and in general the exact mechanism remains in doubt. The data from the HF-treated fibres do, however, reinforce the conclusion that magnesium incorporation is dependent on the presence of silica in the surface layers.

Because any oxides which bond to the mullite layer will be formed from the metal the interfacial bond strength is likely to be high, and mechanical-property data seem to indicate this to be the case [17]. Bonding between these oxides and the metal occurs when valence electrons are shared between metal and substrate, with the oxygen bonds acting as a bridge between them. It would thus appear that the idealized interface, composed of a mechanical continuum (involving coherency on the atomic level) and a chemical discontinuum (requiring the absence of any interdiffusion between constituents [27]) is being approached in this case. It is now interesting to consider this result in the light of a theoretical analysis of oxygen-atom availability.

3.2. Supply of oxygen to the interface

3.2.1. Rate of arrival of atoms

One question that arises in the context of possible interfacial reactions during the relatively rapid infiltration process concerns the supply of oxygen atoms. As molten aluminium has an extraordinarily high affinity for oxygen, it might be imagined that a thin oxide layer would be continually reforming at the infiltration front and that this would be a source of some chemical-species transport to the fibre surface, if only in the form of envelopment with a thin oxide sheath (or possibly as a mechanism for the formation of the postulated $AlO{\cdot}Al_2O_3$ structure [7]). However, with rapid infiltration of a fine fibrous array it is not immediately obvious that the achievable flux of oxygen atoms to the infiltration front would be sufficient to maintain even a monolayer of oxide on the melt surface.

The steady-state concentration profile of oxygen atoms (in the form of O_2 molecules) ahead of the advancing infiltration front is shown schematically in Fig. 6. The reaction rate at the melt–gas interface is assumed to be infinitely high relative to the time scale of the infiltration and diffusion processes. (This is probably acceptable for monolayer formation, but would soon become invalid for multiple layers.) However, even for monolayer formation there will need to be a critical minimum oxygen concentration n_c at the interface in order for neglect of the reaction time to be justifiable, although the magnitude of n_c is probably small. The thickness of the oxygen-depleted layer will be $\delta \sim D/v$, where D is the diffusivity of the oxygen molecules in air at the relevant temperature and v is the velocity of the advancing infiltration front.

The area of fibre surface per unit volume of preform is given by considering the length L of fibre in a volume V_p:

$$\frac{A_{fib}}{V_p} = \frac{2\pi r_{fib} L}{(L\pi r_{fib}^2 / f_{fib})} = \frac{2 f_{fib}}{r_{fib}} \qquad (1)$$

where r_{fib} is the radius of the fibre and f_{fib} is the volume fraction of fibre in the reform. Therefore, in order to maintain an oxide monolayer with an oxygen atom surface density of N it is necessary to supply an oxygen atom flux given by

$$J = \frac{2 N f_{fib} v}{r_{fib}} \qquad (2)$$

This may be compared with the maximum flux diffusing down the concentration gradient in the air being expelled through the fibre network, which is

$$J_{max} \sim D\left[\left(\frac{\partial n}{\partial z'}\right)_{max}\right]_{z'=0} (1 - f_{fib}) \qquad (3)$$

where z' is the distance ahead of the advancing front. The maximum gradient at the interface (which allows maintenance of the oxide layer) depends on what is treated as the minimum oxygen-depleted boundary-layer thickness δ_{min} and on the value of n_c. An upper limit is provided by taking n_c as zero so that

$$J_{max} \sim \frac{D n_{air}}{\delta_{min}} (1 - f_{fib}) \qquad (4)$$

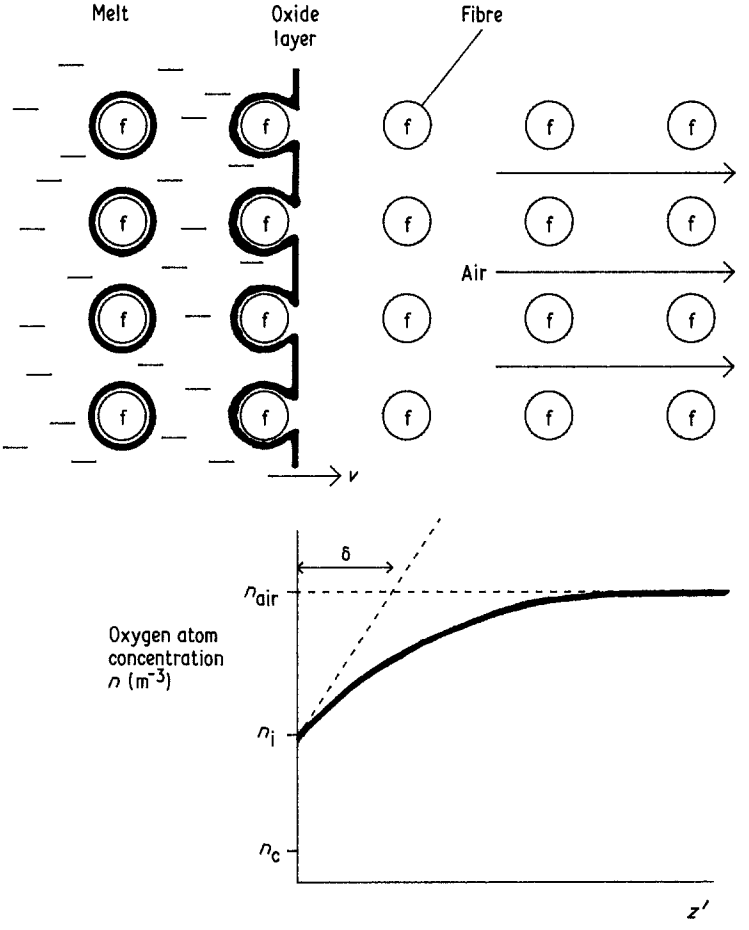

Figure 6 Schematic steady-state concentration profile of oxygen atoms (in the form of O_2 molecules) ahead of the advancing infiltration front.

If this is compared with the required flux given by Equation 2, the condition may be expressed as a maximum velocity of the infiltration front at which an oxide monolayer can be maintained:

$$V_{max} \approx \frac{Dn_{air}r_{fib}}{2Nf_{fib}\delta_{min}}(1-f_{fib}) \qquad (5)$$

There is some uncertainty about the value to employ for δ_{min}, but it would appear dubious to use a figure any lower than the mean free path of the oxygen molecules at the temperature and pressure concerned. If this value is employed then we may complete an assembly of very approximate data [28, 29] for 300° C and atmospheric pressure:

$D \sim 6 \times 10^{-5}$ m^2 sec^{-1} $\quad n_{air} \sim 4 \times 10^{24}$ m^{-3}

$N \sim 3 \times 10^{18}$ m^{-2} $\quad \delta_{min} \sim 4 \times 10^{-7}$ m

giving

$$v_{max} \approx \frac{10^8 r_{fib}}{f_{fib}}(1-f_{fib}) \qquad (6)$$

This suggests that, as might have been expected, monolayer oxide formation can keep pace with rapid infiltration (~ 100 m sec^{-1}), even when the fibres are fine and densely packed. However, it should be noted that several assumptions have been made which will have tended to inflate this figure, and it may well be that the actual oxygen demand (at an infiltration velocity believed to be of the order of 10^{-2} to 10^{-1} m sec^{-1}) is, in fact, not much less than the maximum supply rate. At the least, the figures suggest that formation of a multiple-layer oxide is going to be kinetically unlikely.

3.2.2. Total available oxygen

The difficulty of forming multiple oxygen-containing surface layers is also apparent when another factor is considered, that is the actual quantity of oxygen atoms available for the rig geometry concerned. The number required to form the monolayer is given by $[NV_p(2f_{fib}/r_{fib})]$, while the total initially present in the air contained within the preform is equal to $[V_p(1-f_{fib})n_{air}]$. It

follows that there is a maximum volume fraction of fibres which could be decorated with an oxide monolayer, which is obtained by equating these two expressions to give

$$f_{\text{fib max}} = \left(1 + \frac{2N}{r_{\text{fib}} n_{\text{air}}}\right)^{-1} \quad (7)$$

this being based on the assumption that there will be no time for oxygen to diffuse through the air-escape paths of the die up into the preform. (Indeed it is almost certain that there will be a loss of oxygen atoms through these air-escape paths, and therefore the predicted maximum value of f_{fib} is probably an overestimate). Using the data given above, Equation 7 predicts that oxide monolayers cannot be formed on all fibre surfaces in preforms composed of more than about 50% of fibre by volume; in view of the probable loss of oxygen atoms, the correct figure may well be appreciably lower. It may thus be concluded that not only will it be impossible to form a detectable thickness of any reaction product requiring the incorporation of oxygen onto the fibre surface, but even the formation of a uniform monolayer may be difficult.

4. Conclusions

In composites fabricated by a melt-infiltration process from a preform of δ-alumina fibre, TEM and XPS examinations have shown that the interface between the matrix and the fibre does not exhibit any clearly-identifiable reaction phase. Indeed, it would appear that no exchange of chemical species has taken place on a scale of more than a few atomic layers. In magnesium-containing alloys, bond formation may have involved the generation of a very thin layer into which magnesium ions have penetrated, with the possibility of a relationship between this and a prior layer of mullite on the fibre surface. The depth of magnesium penetration has been estimated at around 1 nm, which is believed to be of the same order as the thickness of a silica-enriched layer on the surface of the fibre. The exact mechanism involved in this exchange is unclear, largely because of uncertainties about the crystallography of the superficial layers, but it may be that the magnesium ions are occupying vacant sites in a defective lattice.

In pure aluminium and magnesium-free alloys, there appears to have been virtually no cation transfer between melt and fibre surface. The bond formed might conceivably have involved the take-up of aluminium oxide (created on the surface of the infiltration front) on to the silica-rich surface, although even this process is in some doubt. In both these cases and those referred to above, any reaction must have taken place on a scale of not more than the few atomic layers on the surface of the fibres.

These results appear to be consistent with other information becoming available on characteristics of the fabrication route. The high pressure appears to ensure intimate physical contact between fibre and matrix, but the infiltration is very rapid (being complete in a time less than 1 sec) and the melt–fibre contact period is also believed to be short (~ 1 min). Furthermore, an order-of-magnitude estimate of the availability of atmospheric oxygen atoms (for incorporation into any fibre/matrix interfacial reaction product formed during infiltration) suggest that these will be in surprisingly short supply. Indeed, limitations on both the rate of delivery and on the total number available within the system suggest that formation of oxygen-containing reaction layers more than a monolayer or so in thickness would not be possible. Of course such limitations would not apply to straight cationic replacement reactions, but these do not appear to have occurred to any significant extent in the systems studied. Finally it may be noted that the microstructural characteristics of these composites would appear to offer excellent performance potential for applications demanding strong interfacial bonding.

Acknowledgements

The authors would like to acknowledge the financial support provided by Imperial Chemical Industries (Mond Division) under a Joint Research Scheme with the University of Surrey. Particular appreciation is expressed to Mr M. G. Bader and Mr P. A. Hubert of the Department of Materials Science and Engineering in the University of Surrey, to Mr J. Dinwoodie of ICI Mond, and to Professor J. D. Birchall of the ICI New Science Group, who have all been of considerable scientific and technical assistance in this work. Thanks are also due to Professor J. E. Castle, director of the Surface Analysis Laboratory in the University of Surrey, for his informative collaboration and advice.

References

1. Data sheet on RF Saffil (ICI Mond Division, Runcorn, Cheshire, UK, 1982).
2. W. R. SYMES and E. RASTETTER, Proceedings of the 24th International Colloquium on Refractories, Aachen, Sept. 1981
3. R. L. MEHAN, *J. Compos. Mater.* 4 (1970) 90.
4. M. J. MOORE, E. FEINGOLD and W. H. SUTTON, ASTM STP 452 (American Society for Testing and Materials, Philadelphia, 1962) p. 90.
5. R. L. MEHAN, ASTM STP 438 (American Society for Testing and Materials, Philadelphia, 1968) p. 29.
6. K. PRABRIPUTALOONG and M. R. PIGGOTT, *Surface Sci.* p. 29. 44 (1974) 585.
7. J. BRENNAN and J. A. PASK, *J. Amer. Ceram. Soc.* **51** (1968) 596.
8. S. K. RHEE, *ibid.* 55 (1972) 300.
9. S. M. WOLF, A. P. LEWIS and J. BROWN, *Chem. Eng. Prog.* **62** (1966) 74.
10. W. KOHLER, *Aluminium* 7 (1975) 443.
11. D. G. GELDERLOOS and K. R. KARASEK, *J. Mater. Sci. Lett.* 3 (1984) 232.
12. A. K. DHINGRA and W. H. KREUGER, "Fiber F.P. Continuous Yarn" (E.I. DuPont de Nemours & Co Inc, Wilmington, Delaware, 1974).
13. C. G. LEVI, G. J. ABBASCHIAN and R. MEHRABIAN, Proceedings of TMS–AIME Meeting, Chicago, Illinois, October 1977, (Met. Soc. AIME, Warrendale, Pennsylvania) p. 37.
14. C. G. LEVI, G. J. ABBASCHIAN and R. MEHRABIAN, *Metall. Trans.* 9A (1978) 697.
15. A. MUNITZ, M. METZGER and R. MEHRABIAN, *ibid.* **10A** (1979) 1491.
16. B. F. QUIGLEY, G. J. ABBASCHIAN, R. WUNDERLIN and R. MEHRABIAN, *ibid.* **13A**, (1982) 93.
17. T. W. CLYNE, M. G. BADER, G. R. CAPPLEMAN and P. A. HUBERT, *J. Mater. Sci.* **20** (1985) 85.
18. W. H. J. VERNON, F. WORMWELL and T. J. NURSE, *J. Chem. Soc.* (1939) 621.
19. J. E. CASTLE and R. H. WEST, *J. Catal.* 57 (1979) 522.
20. J. E. CASTLE, "Analysis of High Temperature Materials", edited by O. van der Biest (Applied Science, London, 1983) p. 141.
21. C. K. JORGENSEN and H. BERTHOU, *Faraday Disc. Chem. Soc.* 44 (1972) 269.
22. D. BRIGGS and M. P. SEAH, "Practical Surface Analysis by Auger and X-ray Photoelectron Spectroscopy" (John Wiley, Chichester, 1983) p. 511.
23. J. E. CASTLE, *Surface Sci.* 68 (1977) 583.
24. J. F. WATTS, PhD thesis, University of Surrey (1982).
25. M. P. SEAH and W. A. DENCH, *Surface Interface Analyses* 1 (1979) 2.
26. W. A. DEER, R. A. HOWIE and J. ZUSSMAN, "Introduction to the rock-forming minerals" (Longman, London, 1966) p. 37.
27. L. J. EBERT and P. KENNARD-WRIGHT, "Composite Materials", 1st edn., Vol. 1 (Academic Press, New York, 1974) p. 31.
28. D. H. GIEGER and D. R. POIRIER, "Transport Phenomena in Metallurgy" (Addison Wesley, Reading, Massachusetts, 1973) p. 468.
29. J. O. HIRSCHFELDER, C. F. CURTISS and R. B. BIRD, "Molecular Theory of Gases and Liquids", (John Wiley, New York, 1954).

Received 16 July
and accepted 31 July 1984